

TRANSIENT ANALYSIS OF LAMINATED PLATES IN THERMAL ENVIRONMENT

Ibtehal Abbas Sadiq, Widad Ibraheem Majeed*

University of Baghdad, Engineering College, Department of Mechanical Engineering, Baghdad, Iraq

*wedad.ibrahim@coeng.uobaghdad.edu.iq

Transient displacement of laminated plates under combined load based on Mantari's displacement field are investigated. The solution is implemented under transient mechanical load (sinusoidal, step and triangular sinusoidal distributed pressures pulse) and thermal buckling for plates with different layer orientation and thickness ratio. Equations of motion based on higher-order theory are derived through Hamilton's principle, and solved using Navier-type solution for simply supported laminated plates. The results are presented for many effective parameters such as the number of laminate and orientation on the dynamic response of plates. Results show the validity of this displacement field in studying response of laminated thick and thin plates under varied transient loading and design parameters.

Keywords: transient, thermal, high shear deformation theory, composite plates

1 INTRODUCTION

Engineering structures, such as a submarine, aircraft, spacecraft, automotive, naval, and rockets are normally exposed to extreme thermal environments and transient loadings, therefore design of plates under static or dynamic loading, is investigated by many researchers using different solution methods, buckling load of laminated plate obtained by [1] for different boundary conditions under different thermal and mechanical loading using Classical plate theory and higher order shear deformation plate theory (HSDT). Transient displacement of laminated plates subjected to thermal and mechanical loading based on classical plate theory studied by [2], also [3] developed Mantari displacement to obtain critical temperature of laminated plates.

Vibration response of thin plate under transient thermal load using Wave-Based Method and Unified formulation developed by [4,5], considering the two theories, Lord-Shulman and Kirchhoff-Love, while [6], derived theoretical models with typical graded thermal distributions considered using classical plate theory, they added thermal and acoustic loadings into the equation of motion at the fluid-structure coupling surface. In [7], vibration of laminated rectangular plate subjected to a hygrothermal environment, analyzed using five theories to derive equations of motion. Studied response of shell under multi load and boundary conditions in thermal environment using FSDT [8,9], developed stability of laminated plate with simply supported boundary conditions under thermal load using a higher order displacement field [10]. Ritz method adopting Classical plate theory, used by [11], to study vibration of laminated plates under different in-plane compressive loadings, while [12], obtained dynamic response of imperfect functionally graded (FG) material thick plates subjected to blast and thermal loads with elastic foundations based on higher order plate theory using two methods Galerkin method and fourth-order Runge-Kutta method also [13], analyzed the vibration and acoustic behavior of FG reinforced nanocomposite laminated plates under thermo-mechanical loading using higher order plate theory and Rayleigh integral method while [14], investigated responses of laminated beams under a moving load with thermal effects, using Ritz theory.

Numerical analysis used by [15], to study the effect of thermal environment on free vibration behavior of laminated plates developing finite element model based on first order theory also [16], used finite element model to study dynamic response of functionally graded plates in thermal environment, while [17], studied characteristics of free vibration and the buckling (mechanical and/or thermal) for laminated composite flat and curved panels numerically using ANSYS program, also, [18], used a stochastic finite element model to analyze the free and forced vibration response of the laminated plate under a uniform thermal load. In [19], presented response of a layered annular plate with damages under static or dynamic thermal model using finite difference and finite element analyses based on classical theory.

In [20] developed a new finite element model for shells and plates for static and dynamic analysis, also [21] studied thermomechanical response of shells and plates using finite element model with high-order and first-order shell theory. Finite element model for vibrations of laminated plate rest on elastic boundary subjected to thermal loading, established by [22], while in [23] investigated stress and deformation for functionally graded cylinder using Finite Difference Method based on First-order shear deformation theory. A review of governing equations on properties of FG materials as well as thermoelastic response of materials provided by [24]. The literature review shows researches, which analyze the combined problem of thermal buckling, as well as dynamic loading for composite plates, shells and beams, based on different displacement functions, and solved by many methods such as analytic, approximate and numerical, which influence the accuracy of results, while response of these structural elements is affected by many design parameters. Response of laminated thick and thin plates under dynamic and thermal loading is investigated in present work using Mantari's displacement field for first time.

2 METHODOLOGY

In present work, Mantari' s displacement field which its aim, is to develop a plate model that its mechanical behavior close to the three-dimension solutions.

In [25] with 'm=0.5' value is used to obtain response for laminated plates under transient load and thermal load (as a ratio of critical thermal temperature), but this displacement is modified by [3], to get critical temperature for these plates with 'm=0.05':

$$\begin{aligned}\bar{u}_{(x,y,z)} &= u_{(x,y)} + z \left[\frac{\pi}{h} m * \theta 1 - \frac{\partial w}{\partial x} \right] + \sin \left(\frac{\pi z}{h} \right) e^{m * \cos \left(\frac{\pi z}{h} \right)} \theta 1 \\ \bar{v}_{(x,y,z)} &= v_{(x,y)} + z \left[\frac{\pi}{h} m * \theta 2 - \frac{\partial w}{\partial y} \right] + \sin \left(\frac{\pi z}{h} \right) e^{m * \cos \left(\frac{\pi z}{h} \right)} * \theta 2 \\ \bar{w}_{(x,y,z)} &= w_{(x,y)}\end{aligned}\quad (1)$$

The strain-displacement relations:

$$\begin{aligned}\varepsilon_{xx} &= \varepsilon_{xx}^0 + z \varepsilon_{xx}^1 + \sin \left(\frac{\pi z}{h} \right) e^{m * \cos \left(\frac{\pi z}{h} \right)} \varepsilon_{xx}^2 \\ \varepsilon_{yy} &= \varepsilon_{yy}^0 + z \varepsilon_{yy}^1 + \sin \left(\frac{\pi z}{h} \right) e^{m * \cos \left(\frac{\pi z}{h} \right)} \varepsilon_{yy}^2 \\ \gamma_{xy} &= \gamma_{xy}^0 + z \gamma_{xy}^1 + \sin \left(\frac{\pi z}{h} \right) e^{m * \cos \left(\frac{\pi z}{h} \right)} \gamma_{xy}^2 \\ \gamma_{xz} &= \gamma_{xz}^0 + \frac{\pi}{h} \left(\cos \left(\frac{\pi z}{h} \right) + m * \sin^2 \left(\frac{\pi z}{h} \right) \right) e^{m * \cos \left(\frac{\pi z}{h} \right)} \gamma_{xz}^3 \\ \gamma_{yz} &= \gamma_{yz}^0 + \frac{\pi}{h} \left(\cos \left(\frac{\pi z}{h} \right) + m * \sin^2 \left(\frac{\pi z}{h} \right) \right) e^{m * \cos \left(\frac{\pi z}{h} \right)} \gamma_{yz}^3\end{aligned}\quad (2)$$

2.1 HAMILTONS PRINCIPLE

The equations of motion are derived using energy method as shown below [26]:

$$0 = \int_0^t \delta U + \delta V - \delta K \quad (3)$$

The virtual strain energy δU is:

$$\delta U = \int_A \left\{ \int_{-h/2}^{h/2} \left[\sigma_{xx} \delta \varepsilon_{xx} + \sigma_{yy} \delta \varepsilon_{yy} + \sigma_{xy} \delta \varepsilon_{xy} + \sigma_{xz} \delta \varepsilon_{xz} + \sigma_{yz} \delta \varepsilon_{yz} \right] dz \right\} dA$$

Substituting Eqs. (1 and 2) into Eq. (3) to give:

$$\begin{aligned}\delta U &= \int_A \left\{ \int_{-h/2}^{h/2} \left[\sigma_{xx} \delta \left(\varepsilon_{xx}^0 + z \varepsilon_{xx}^1 + \sin \left(\frac{\pi z}{h} \right) e^{m * \cos \left(\frac{\pi z}{h} \right)} \varepsilon_{xx}^2 \right) + \sigma_{yy} \delta \left(\varepsilon_{yy}^0 + z \varepsilon_{yy}^1 + \sin \left(\frac{\pi z}{h} \right) e^{m * \cos \left(\frac{\pi z}{h} \right)} * \varepsilon_{yy}^2 \right) \right. \right. \\ &\quad + \sigma_{xy} \delta \left(\gamma_{xy}^0 + z \gamma_{xy}^1 + \sin \left(\frac{\pi z}{h} \right) e^{m * \cos \left(\frac{\pi z}{h} \right)} * \gamma_{xy}^2 \right) \\ &\quad + \sigma_{xz} \delta \left(\gamma_{xz}^0 + \frac{\pi}{h} \left(\cos \left(\frac{\pi z}{h} \right) - m * \sin^2 \left(\frac{\pi z}{h} \right) \right) e^{m * \cos \left(\frac{\pi z}{h} \right)} * \gamma_{xz}^3 \right) \\ &\quad \left. \left. + \sigma_{yz} \delta \left(\gamma_{yz}^0 + \frac{\pi}{h} \left(\cos \left(\frac{\pi z}{h} \right) + m * \sin^2 \left(\frac{\pi z}{h} \right) \right) e^{m * \cos \left(\frac{\pi z}{h} \right)} * \gamma_{yz}^3 \right) \right] dz \right\} dA\end{aligned}$$

$$\begin{aligned}\delta U &= \int_A \left[N_1 \delta \varepsilon_{xx}^0 + M_1 \delta \varepsilon_{xx}^1 + P_1 \delta \varepsilon_{xx}^2 + N_2 \delta \varepsilon_{yy}^0 + M_2 \delta \varepsilon_{yy}^1 + P_2 \delta \varepsilon_{yy}^2 + N_6 \delta \gamma_{xy}^0 + M_6 \delta \gamma_{xy}^1 + P_6 \delta \gamma_{xy}^2 + Q_2 \delta \gamma_{yz}^0 + K_2 \delta \gamma_{yz}^3 \right. \\ &\quad \left. + Q_1 \delta \gamma_{xz}^0 + K_1 \delta \gamma_{xz}^3 \right] dA\end{aligned}$$

Work done by external applied loads δV is:

$$\delta V = \int_{\Omega} \left\{ N_x^T \delta \left(\frac{\partial w}{\partial x} \right)^2 + N_y^T \delta \left(\frac{\partial w}{\partial y} \right)^2 + q * w \right\} dx dy$$

The virtual Kinetic energy δK is:

$$\delta K = \int_V \rho [u\delta u + v\delta v + w\delta w] dV$$

$$\begin{aligned} \delta K = \int_t \int_A & \left[\left(I_2 \frac{\partial \ddot{w}_0}{\partial x} - I_1 \ddot{u}_0 - \left(\frac{m\pi}{h} I_2 + I_4 \right) \ddot{\theta}_1 \right) \delta u_0 + \left(I_2 \frac{\partial \ddot{w}_0}{\partial y} - I_1 \ddot{v}_0 - \left(\frac{m\pi}{h} I_2 + I_4 \right) \ddot{\theta}_2 \right) \delta v_0 \right. \\ & + \left(I_3 \frac{\partial^2 \ddot{w}_0}{\partial x^2} - I_2 \frac{\partial \ddot{u}_0}{\partial x} - \left(\frac{m\pi}{h} I_2 + I_5 \right) \frac{\partial \ddot{\theta}_1}{\partial x} - I_2 \frac{\partial \ddot{v}_0}{\partial y} + \left(\frac{m\pi}{h} I_2 + I_5 \right) \frac{\partial \ddot{\theta}_2}{\partial y} + I_3 \frac{\partial^2 \ddot{w}_0}{\partial y^2} + I_1 \ddot{w}_0 \right) \delta w_0 \\ & + \left(\frac{m\pi}{h} I_3 \ddot{w}_0 - \left(\frac{m\pi}{h} I_2 + I_4 \right) \ddot{u}_0 + I_5 \frac{\partial \ddot{w}_0}{\partial x} + \left(2 \frac{m\pi}{h} I_5 + \left(\frac{m\pi}{h} \right)^2 I_3 + I_6 \right) \ddot{\theta}_1 \right) \delta \theta_1 \\ & \left. + \left(\frac{m\pi}{h} I_3 \ddot{w}_0 - \left(\frac{m\pi}{h} I_2 + I_4 \right) \ddot{v}_0 + I_5 \frac{\partial \ddot{w}_0}{\partial y} + \left(2 \frac{m\pi}{h} I_5 + \left(\frac{m\pi}{h} \right)^2 I_3 + I_6 \right) \ddot{\theta}_2 \right) \delta \theta_2 \right] dA dt \end{aligned}$$

$$I_i = \int_{-h/2}^{h/2} \rho \left(1, z, z^2, \sin \left(\frac{\pi z}{h} \right) e^{m \cdot \cos \left(\frac{\pi z}{h} \right)}, z * \sin \left(\frac{\pi z}{h} \right) e^{m \cdot \cos \left(\frac{\pi z}{h} \right)}, \sin^2 \left(\frac{\pi z}{h} \right) e^{m \cdot \cos \left(\frac{\pi z}{h} \right)} \right) dz$$

where: (i = 1,2,3,4,5,6)

2.2 EQUATIONS OF MOTION

From Eq. (3) five equations of motion are derived as follows:

$$\delta u_0 : \frac{\partial N1}{\partial x} + \frac{\partial N6}{\partial y} = I_1 \ddot{u}_0 - I_2 \frac{\partial \ddot{w}_0}{\partial x} - (gI_2 + I_4) \theta_1$$

$$\delta v_0 : \frac{\partial N2}{\partial y} + \frac{\partial N6}{\partial x} = I_1 \ddot{v}_0 - I_2 \frac{\partial \ddot{w}_0}{\partial y} - (gI_2 + I_4) \theta_2$$

$$\begin{aligned} \delta w_0 : & \frac{\partial^2 M1}{\partial x^2} + \frac{\partial^2 M2}{\partial y^2} + 2 \frac{\partial^2 M6}{\partial x \partial y} + N_x^T \left(\frac{\partial^2 w}{\partial x^2} \right) + N_y^T \left(\frac{\partial^2 w}{\partial y^2} \right) \\ & = I_2 \frac{\partial \ddot{u}_0}{\partial x} + I_2 \frac{\partial \ddot{v}_0}{\partial y} - I_3 \frac{\partial^2 \ddot{w}_0}{\partial x^2} + (gI_2 + I_5) \frac{\partial \ddot{\theta}_1}{\partial x} + (gI_2 + I_5) \frac{\partial \ddot{\theta}_2}{\partial y} - I_3 \frac{\partial^2 \ddot{w}_0}{\partial y^2} - \ddot{w}_0 \end{aligned}$$

$$\delta \theta_1 : g \frac{\partial M1}{\partial x} + g \frac{\partial M6}{\partial y} + \frac{\partial P1}{\partial x} + \frac{\partial P6}{\partial y} + gQ_1 + K_1 = (2gI_5 + g^2 I_3 + I_6) \ddot{\theta}_1 + (gI_2 + I_5) \ddot{u}_0 - I_5 \frac{\partial \ddot{w}_0}{\partial x} - gI_3 \ddot{w}_0$$

$$\delta \theta_2 : g \frac{\partial M2}{\partial y} + g \frac{\partial M6}{\partial x} + \frac{\partial P2}{\partial y} + \frac{\partial P6}{\partial x} + gQ_2 + K_2 = (2gI_5 + g^2 I_3 + I_6) \ddot{\theta}_2 + (gI_2 + I_5) \ddot{v}_0 - I_5 \frac{\partial \ddot{w}_0}{\partial y} - gI_3 \ddot{w}_0 \quad (4)$$

Resultant forces are given by:

$$\begin{Bmatrix} Q_1 \\ Q_2 \\ K_1 \\ K_2 \end{Bmatrix} = \begin{bmatrix} A_{55} & A_{54} & J_{11} & J_{12} \\ A_{45} & A_{44} & J_{21} & J_{22} \\ J_{11} & J_{12} & L_{11} & L_{12} \\ J_{21} & J_{22} & L_{21} & L_{22} \end{bmatrix} \begin{Bmatrix} \varepsilon_{xz}^0 \\ \varepsilon_{yz}^0 \\ \varepsilon_{xz}^3 \\ \varepsilon_{yz}^3 \end{Bmatrix}$$

$$\begin{Bmatrix} N_1 \\ N_2 \\ N_6 \\ M_1 \\ M_2 \\ M_6 \\ P_1 \\ P_2 \\ P_6 \end{Bmatrix} = \begin{bmatrix} A_{11} & A_{12} & A_{16} & B_{11} & B_{12} & B_{16} & E_{11} & E_{12} & E_{16} \\ A_{21} & A_{22} & A_{26} & B_{21} & B_{22} & B_{26} & E_{21} & E_{22} & E_{26} \\ A_{61} & A_{62} & A_{66} & B_{61} & B_{62} & B_{66} & E_{61} & E_{62} & E_{66} \\ B_{11} & B_{12} & B_{16} & D_{11} & D_{12} & D_{16} & F_{11} & F_{12} & F_{16} \\ B_{21} & B_{22} & B_{26} & D_{21} & D_{22} & D_{26} & F_{21} & F_{22} & F_{26} \\ B_{61} & B_{62} & B_{66} & D_{61} & D_{62} & D_{66} & F_{61} & F_{62} & F_{66} \\ E_{11} & E_{12} & E_{16} & F_{11} & F_{12} & F_{16} & H_{11} & H_{12} & H_{16} \\ E_{21} & E_{22} & E_{26} & F_{21} & F_{22} & F_{26} & H_{21} & H_{22} & H_{26} \\ E_{61} & E_{62} & E_{66} & F_{61} & F_{62} & F_{66} & H_{61} & H_{62} & H_{66} \end{bmatrix} \begin{Bmatrix} \varepsilon_{xx}^0 \\ \varepsilon_{yy}^0 \\ \varepsilon_{xy}^0 \\ \varepsilon_{xx}^1 \\ \varepsilon_{yy}^1 \\ \varepsilon_{xy}^1 \\ \varepsilon_{xx}^2 \\ \varepsilon_{yy}^2 \\ \varepsilon_{xy}^2 \end{Bmatrix}$$

$$\begin{Bmatrix} N_x^T \\ N_y^T \\ N_{xy}^T \end{Bmatrix} = \sum_{k=1}^N \int_{z^k}^{z^{k+1}} \begin{bmatrix} Q_{11} & Q_{12} & Q_{16} \\ Q_{12} & Q_{22} & Q_{26} \\ Q_{16} & Q_{26} & Q_{66} \end{bmatrix} \begin{Bmatrix} \alpha_{xx} \\ \alpha_{yy} \\ 2\alpha_{xy} \end{Bmatrix} \Delta T dz$$

where: $\Delta T = T - T_{ref}$.

Where:

$$(A_{ij}, B_{ij}, D_{ij}, E_{ij}, F_{ij}, H_{ij}) = \int_{-h/2}^{h/2} Q_{ij} \left(1, z, z^2, \sin\left(\frac{\pi z}{h}\right) e^{m \cdot \cos\left(\frac{\pi z}{h}\right)}, z * \sin\left(\frac{\pi z}{h}\right) e^{m \cdot \cos\left(\frac{\pi z}{h}\right)}, \sin^2\left(\frac{\pi z}{h}\right) e^{m \cdot \cos\left(\frac{\pi z}{h}\right)} \right) dz, \\ (i = 1, 2, 4, 5, 6)$$

$$J_{ij} = \int_{-h/2}^{h/2} Q_{ij} \frac{\pi}{h} \left(\cos\left(\frac{\pi z}{h}\right) - m \sin^2\left(\frac{\pi z}{h}\right) e^{m \cdot \cos\left(\frac{\pi z}{h}\right)} \right) dz$$

$$L_{ij} = \int_{-h/2}^{h/2} Q_{ij} \frac{\pi^2}{h^2} \left(\cos\left(\frac{\pi z}{h}\right) - m \sin^2\left(\frac{\pi z}{h}\right) e^{m \cdot \cos\left(\frac{\pi z}{h}\right)} \right)^2 dz, (i = 1, 2)$$

The stress-strain relationship of lamina in a plane stress state is [26]:

$$\begin{Bmatrix} \sigma_{xx} \\ \sigma_{yy} \\ \sigma_{xy} \\ \sigma_{xz} \\ \sigma_{yz} \end{Bmatrix} = \begin{bmatrix} Q_{11} & Q_{12} & Q_{16} & 0 & 0 \\ Q_{21} & Q_{22} & Q_{26} & 0 & 0 \\ Q_{61} & Q_{62} & Q_{66} & 0 & 0 \\ 0 & 0 & 0 & Q_{55} & Q_{54} \\ 0 & 0 & 0 & Q_{45} & Q_{44} \end{bmatrix} \begin{Bmatrix} \varepsilon_{xx} \\ \varepsilon_{yy} \\ \gamma_{xy} \\ \gamma_{xz} \\ \gamma_{yz} \end{Bmatrix}$$

Navier's series for simply supported cross-ply and angle laminates (with a and b dimensions), are given in [26].

2.3 TRANSIENT SOLUTION

Principal mode method is used to calculate response of plate under transient and thermal load, and taking into consideration orthogonality condition of modes, as follows [27]:

$$(\omega_{mn}^2 - \omega_{sr}^2) \int_0^a \int_0^b \left\{ [I_1 U_{mn} + I_2 (2g\theta_{1mn} - \frac{\partial w_{mn}}{\partial x}) + 2I_4 \theta_{1mn} + I_5 \theta_{1mn}] U_{sr} + [I_1 V_{mn} + I_2 (2g\theta_{2mn} - \frac{\partial w_{mn}}{\partial y}) + 2I_4 \theta_{2mn} + I_5 \theta_{2mn}] V_{sr} + [I_1 W_{mn} + I_2 (\frac{\partial U_{mn}}{\partial x} + \frac{\partial V_{mn}}{\partial y}) + I_3 (g\theta_{1mn} + \frac{\partial \theta_{1mn}}{\partial x} - \frac{\partial^2 w_{mn}}{\partial x^2} - \frac{\partial^2 w_{mn}}{\partial y^2}) + I_5 (\frac{\partial \theta_{1mn}}{\partial x} + \frac{\partial \theta_{2mn}}{\partial y})] W_{sr} + [2gI_2 U_{mn} + I_3 (g^2 \theta_{1mn} + g \frac{\partial w}{\partial x}) + 2I_4 U_{mn} + I_5 (2g\theta_{1mn} + \frac{\partial w_{mn}}{\partial x} + U_{mn})] \theta_{1sr} + [2gI_2 V_{mn} + I_3 (g^2 \theta_{2mn} + g \frac{\partial w_{mn}}{\partial y}) + 2I_4 V_{mn} + I_5 (2g\theta_{2mn} + \frac{\partial w_{mn}}{\partial y} + V_{mn})] \theta_{2sr} \right\} dx dy = 0 \quad (5)$$

Generalized forces are determined by making use of the orthogonality condition as:

$$f_{mn}(t) = \frac{\int_0^a \int_0^b (q * W_{mn}) dx dy}{N_{mn}} \quad (6)$$

Where:

$$N_{mn} = \int_0^a \int_0^b \left\{ I_1 [U_{mn}^2 + V_{mn}^2 + W_{mn}^2] + I_2 \left[W_{mn} \frac{\partial V_{mn}}{\partial y} + W_{mn} \frac{\partial U_{mn}}{\partial x} + 2gV_{mn}\theta_{2mn} + 2gU_{mn}\theta_{1mn} - U_{mn} \frac{\partial w_{mn}}{\partial x} - V_{mn} \frac{\partial w_{mn}}{\partial y} \right] + I_3 \left[g\theta_{2mn} \frac{\partial w_{mn}}{\partial y} + g^2 \theta_{2mn}^2 + g\theta_{1mn} \frac{\partial w_{mn}}{\partial x} + g^2 \theta_{1mn}^2 + gW_{mn} \frac{\partial \theta_{2mn}}{\partial y} + gW_{mn} \frac{\partial \theta_{1mn}}{\partial x} - W_{mn} \frac{\partial^2 w_{mn}}{\partial y^2} - W_{mn} \frac{\partial^2 w_{mn}}{\partial x^2} \right] + 2I_4 [U_{mn}\theta_{1mn} + V_{mn}\theta_{2mn}] + I_5 \left[2g\theta_{2mn}^2 + 2g\theta_{1mn}^2 + \theta_{1mn} \frac{\partial w_{mn}}{\partial x} + \theta_{2mn} \frac{\partial w_{mn}}{\partial y} + W_{mn} \frac{\partial \theta_{1mn}}{\partial x} + W_{mn} \frac{\partial \theta_{2mn}}{\partial y} + U_{mn}\theta_{1mn} + V_{mn}\theta_{2mn} \right] \right\} dx dy \\ u_{i(x,y)} = \sum_{m=n=1}^{\infty} U_{imn(x,y)} T_{imn(t)} \quad (7)$$

Where (U_{imn} for $i = 1, 2, 3, 4, 5$) are the plate modes, while $T_{mn(t)}$ is an unknown time function. Substituting Eq. (7) in Eq. (4) results in:

$$\ddot{T}_{mn} + \omega_{mn}^2 T_{mn} = f_{mn} \quad (8)$$

For zero initial conditions, the solution of Eq. (8) is given by [21]:

$$T_{mn}(t) = \frac{1}{\omega_{mn}} \int_0^t f_{mn}(\tau) \sin \omega_{mn}(k)(t - \tau) d\tau \quad (9)$$

Response of plate under a load $q(x,y,t) = q_0 f_3(x,y) F(t)$, ($m=n=1$), can be presented as:

$$\begin{Bmatrix} u \\ v \\ w \\ \theta_1 \\ \theta_2 \end{Bmatrix} = \sum_{k=1}^5 \frac{q_0}{J_{mn(k)} \omega_{mn(k)}} \begin{Bmatrix} U_{mn(k)} \\ V_{mn(k)} \\ f_3 \\ \theta_{1mn(k)} \\ \theta_{2mn(k)} \end{Bmatrix} \int_0^t F(\tau) \sin \omega_{mn}(k)(t - \tau) d\tau \quad (10)$$

The force function $F(t)$ for sin, step and triangle pulse respectively are [27]:

$$F(t) = \begin{cases} \sin(\pi t/t_1) & 0 \leq t \leq t_1 \\ 0 & t > t_1 \end{cases}$$

$$F(t) = \begin{cases} 1 & 0 \leq t \leq t_1 \\ 0 & t > t_1 \end{cases}$$

$$F(t) = \begin{cases} (1 - t/t_1) & 0 \leq t \leq t_1 \\ 0 & t > t_1 \end{cases}$$

3 RESULTS AND DISCUSSION

3.1 Verification Study

To verify the present model, results of response of laminated plate are compared with [28] for the angle-ply (45°/-45°) square plate ($a = b = 10h$). It is obvious that this displacement field is effective to study the dynamic response and stress components of thick and thin plates under different dynamic load; also, the discrepancy is very small since [28] used HSDT with different function as shown in Fig. 1.

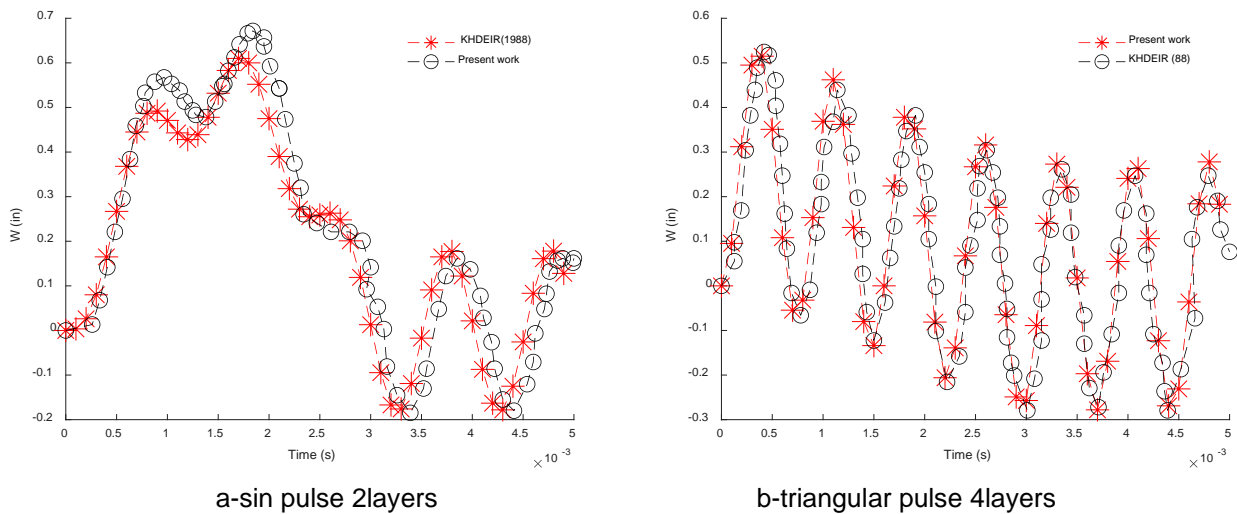


Fig. 1. Verification of central displacement for angle plate [±45]

3.2 Results for cross-ply

Forced vibration analysis for cross and angle plates under thermal loading, solution is implemented based on Mantari function under thermomechanical loading (sinusoidal, step and triangular sinusoidally distributed pulse) using Matlab 2019b.

Two material model are used:

First model (1): $\alpha_1 = 1; \alpha_2 = 3; E_1 = 172.369 \text{ GPa}; E_2 = 6.895 \text{ GPa}; E_3 = E_2; \mu_{12} = 0.25; \mu_{13} = 0; \mu_{23} = 0; G_{12} = 3.448 \text{ GPa}; G_{13} = G_{12}; G_{23} = 1.379 \text{ GPa}; \rho = 1603.03 \text{ kg/m}^3$.

Second model (2): $\alpha_1 = 1; \alpha_2 = 3; E_2 = 21 \text{ GPa}; E_1 = 25 * E_2; E_3 = E_2; \mu_{12} = 0.25; \mu_{13} = 0; \mu_{23} = 0; G_{12} = 0.5 * E_2; G_{13} = G_{12}; G_{23} = 0.2 * E_2; \rho = 800 \text{ kg/m}^3$.

Fig. 2 shows the response of simply supported anti symmetric cross plates under transient mechanical load with thermal buckling, from which the transverse displacement component under sin pulse is the largest compared with step pulse ($T_c = 0.03166155 \text{ C}^\circ$ for two cross ply, noting that $T_{ref} = 0$), for sinusoidal load use $q = 68.9476 \text{ Mpa}$, $a=b$, $= 0.762$, $h=0.1524 \text{ (m)}$, with material model (1).

Simply supported with material model (1) symmetric cross plates response is investigated under transient mechanical load and thermal buckling (ratio of T_c) is plotted in Fig.3, from which the transverse displacement component under sine pulse is greater than step pulse (increases when ratio of applied T_c increased), while effect of these loads on non dimensionalized normal stress component (σ_1) are shown in Fig. 4, also it is noticed that the plate behavior is not changed.

Fig. 5, shows a comparison for response of simply supported four layers symmetric and anti-symmetric cross plates under sine and triangle pulse load with thermal buckling, from which the response of anti-symmetric plate is better than symmetric plate although its T_c is larger indicating that the cross plies are most effective under transverse load $a=b= 0.762$; $h= 0.1524$ (m) with material model (1). For sinusoidal load use $q = 68.9476$ (Mpa); for symmetric layers $T_c = 0.009673$, and $T_c = 0.011433$ for anti-symmetric layers, noting that $T_{ref.} = 0$.

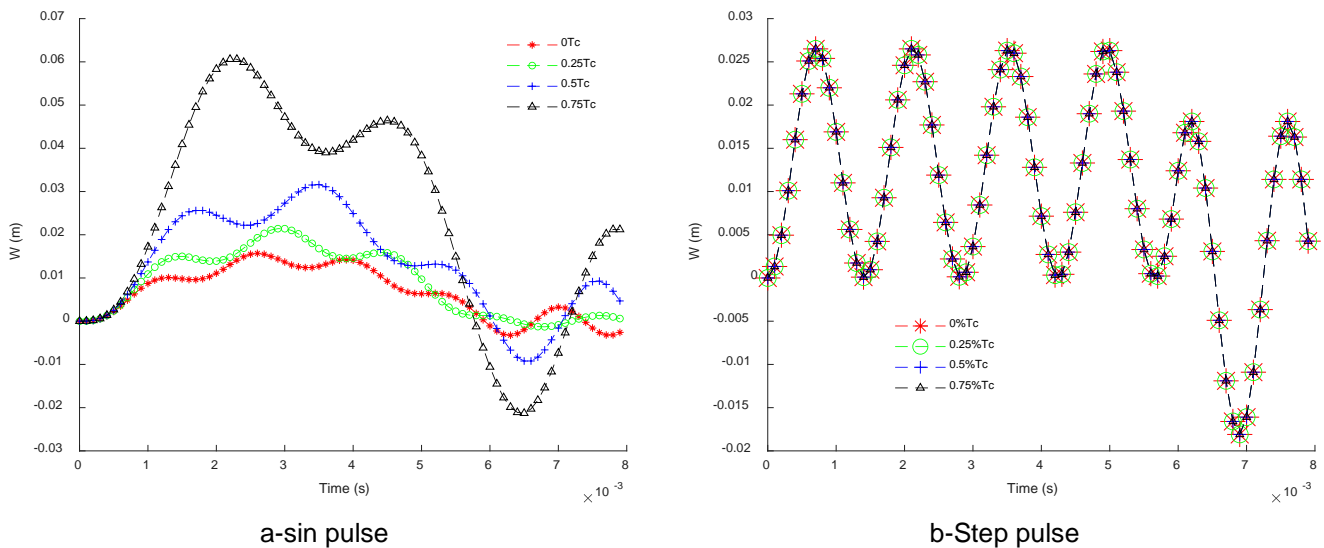


Fig. 2. Center deflection for [0/90] square plate under mechanical pulse and (% T_c)

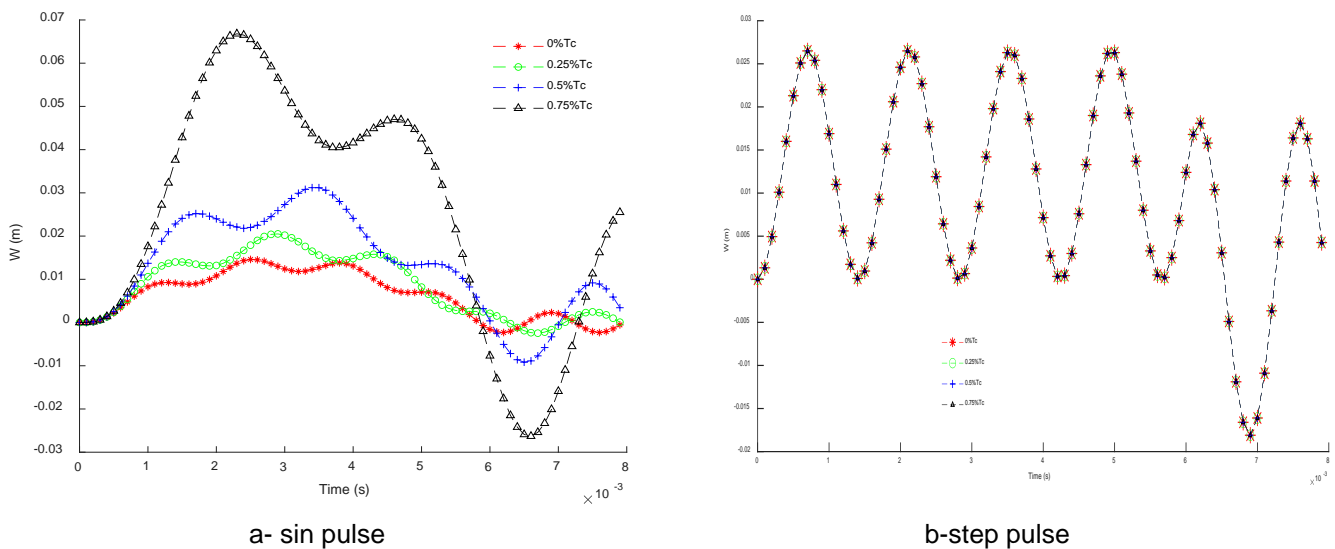
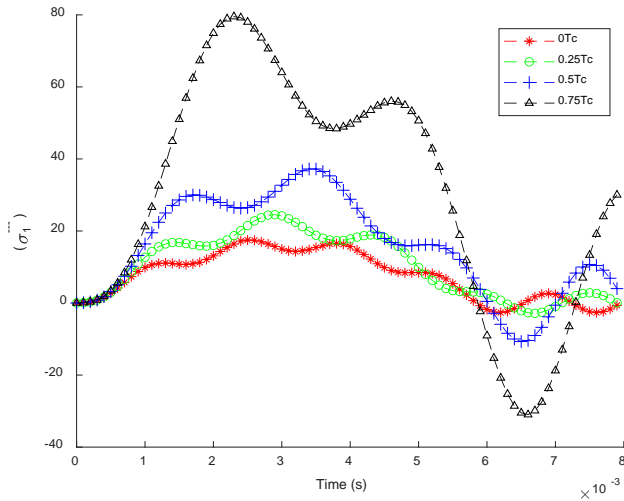
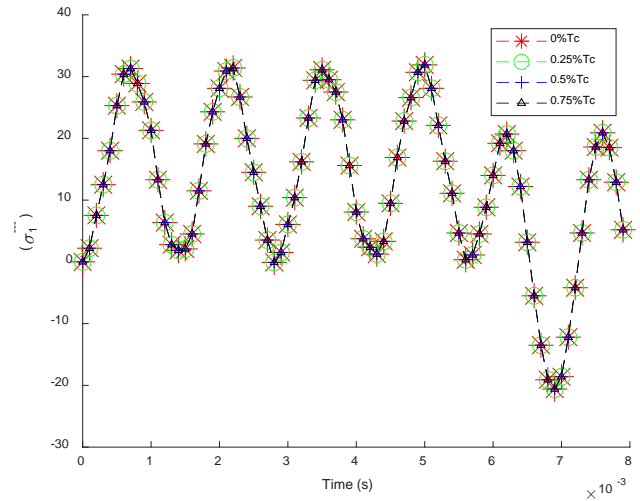


Fig. 3. Center deflection for [0/90/90/0] square plate under mechanical pulse and (% T_c)

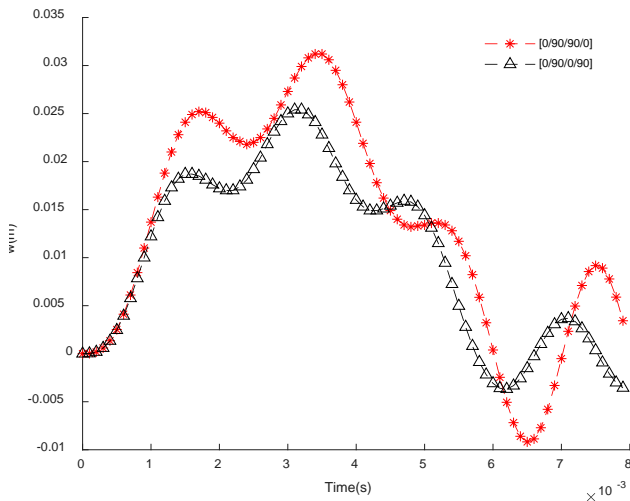


a- sin pulse

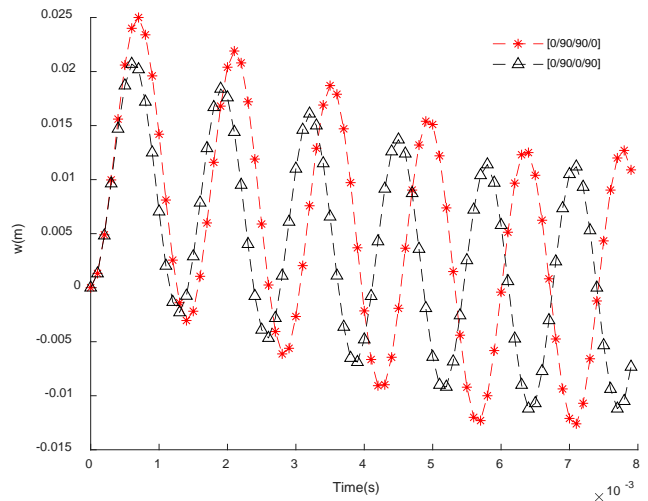


b-step pulse

Fig. 4. stress for [0/90/90/0] square plate under mechanical pulse and (%Tc)



a-sin pulse



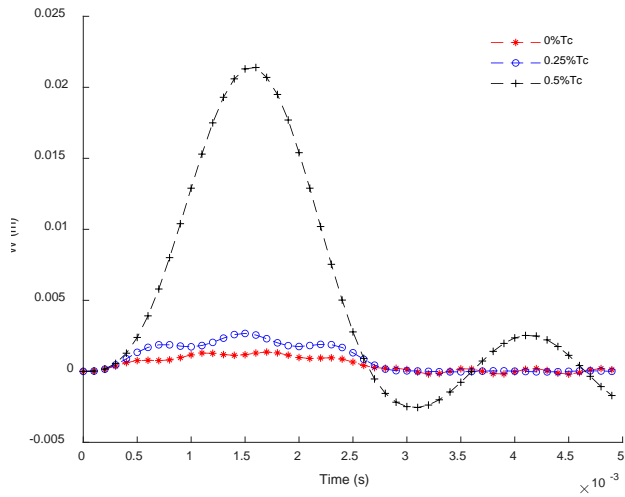
b- triangular pulse

Fig. 5. Central deflection for 4 layers cross ply square plate under mechanical pulse and (0.5%Tc)

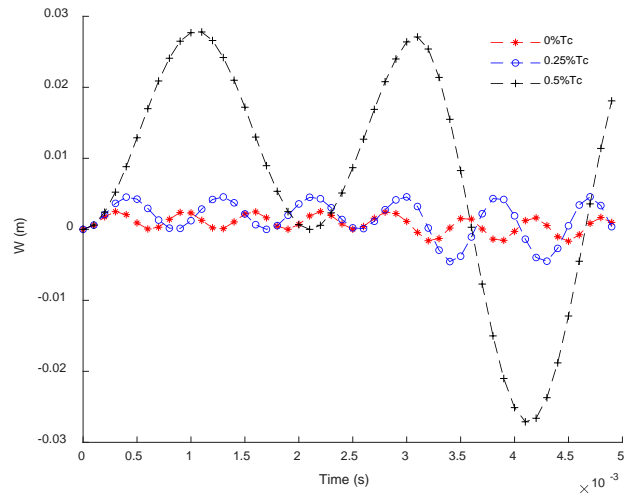
3.3 Results for angle-ply

Angle plates response is investigated under thermo mechanical loading is plotted in Fig.6 for simply supported $[\pm 45]$, larger transverse displacement component is under step pulse and increases when ratio of applied T_{cr} increased, same behavior is obtained for 4 layers angle plates as shown in Fig. 7, but with smaller magnitudes since stiffness is better.

Transverse load is $q = 1 \text{ MN/m}^2$ and $a=b = 25$, $h=1$ with material model (2) and $T_c = 0.0008227 \text{ C}^\circ$ for two layers and $T_c = 0.001796 \text{ C}^\circ$ for four layers, noting that $T_{ref} = 0$.

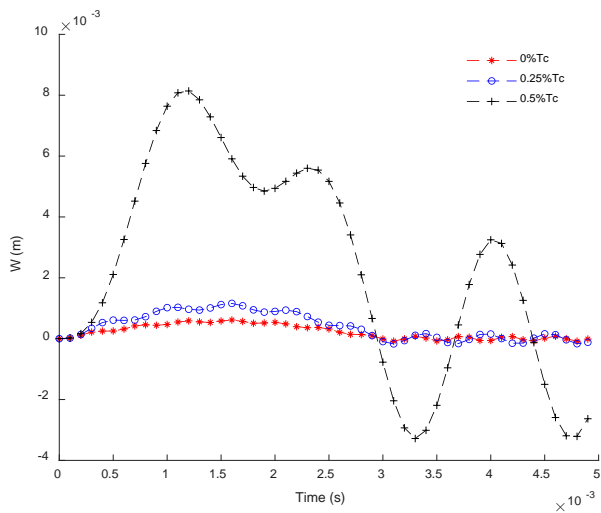


a-sin pulse

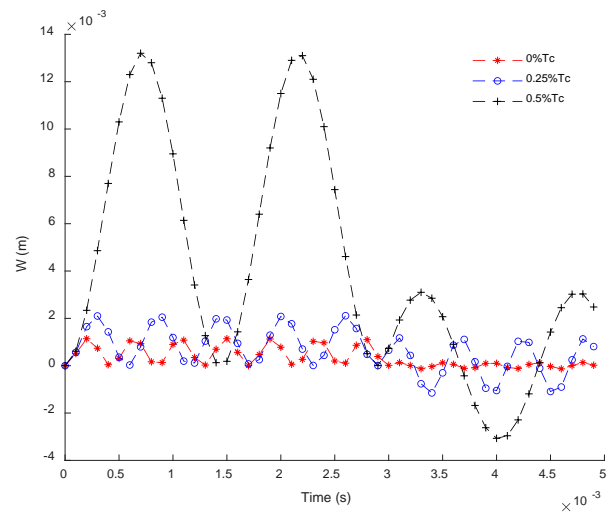


b-step pulse

Fig. 6. Center deflection for [45/-45] square plate under mechanical pulse and (%Tc)



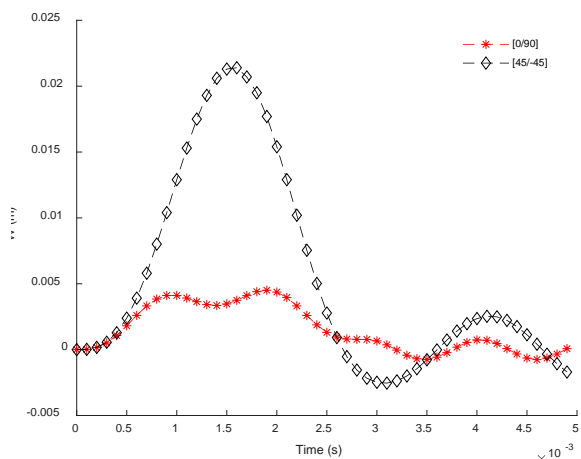
a-sin pulse



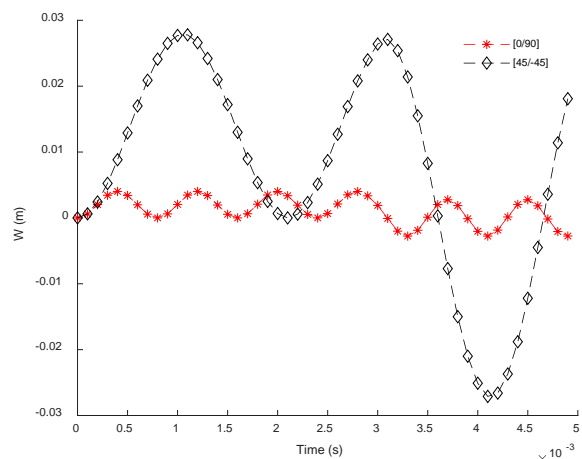
b-step pulse

Fig. 7. Center deflection for [45/-45/45/-45] square plate under mechanical pulse and (%Tc)

Response comparison between 2 and 4 layers cross ply and angle ply under thermo-mechanical loading, shown in Fig. 8 and Fig. 9 respectively, from which it is obvious that response of cross plies better than angle plies although it's Tc is smaller indicating that the most effective load is transverse mechanical. For [0/90] Tc = 0.000512 and for [0/90/0/90], Tc = 0.001041, (mechanical properties are same for angle plies).



a- sin pulse



b-step pulse

Fig. 8. Center deflection for 2layers square plate under mechanical pulse and (0.5%Tc)

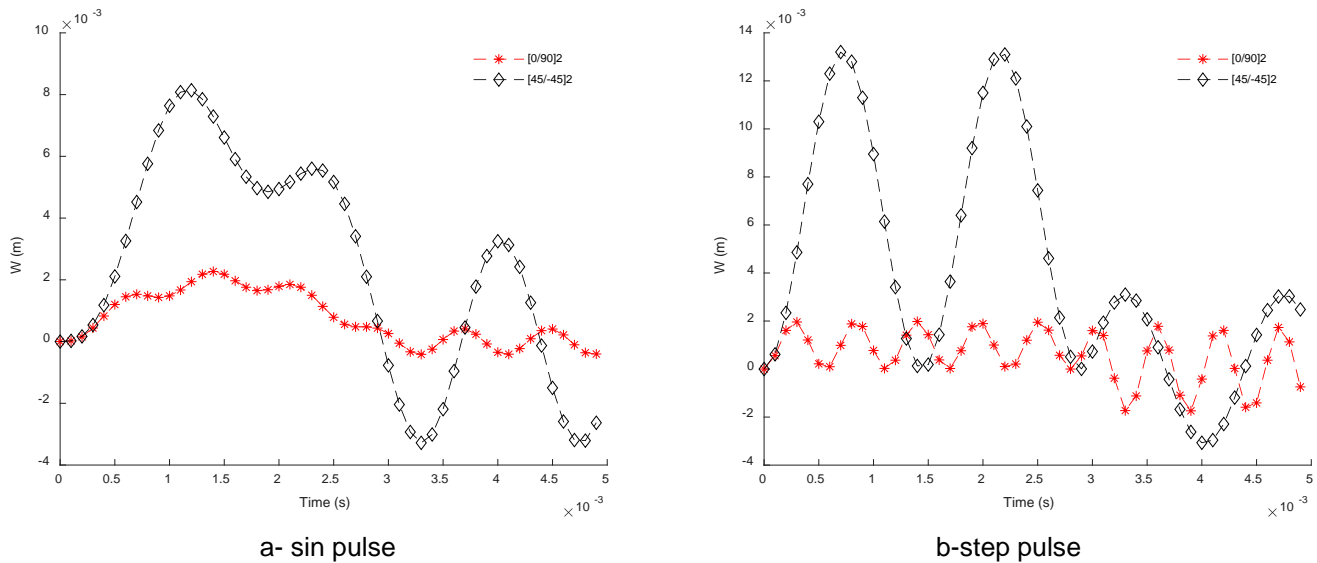


Fig. 9. Center deflection for 4 layers square plate under mechanical pulse and (0.5%Tc)

4 CONCLUSIONS

The novelty includes using Mantari function to analyze the dynamic response of angle and cross-ply laminated plates under uniform temperature distribution. Results show the validity of displacement function in investigating deformation of thick and thin laminated plates under combined (sine, step and triangular pulse) and thermal loading with changing some design parameters, also the discrepancy is very small when compared with those obtained by researchers used different functions.

5 REFERENCES

- [1] Jameel A., Sadiq I. and Nsaif H. (2012). Buckling analysis of composite plates under thermal and mechanical loading. *Journal of Engineering*, vol. 18, no. 12, 1365-1390.
- [2] Jamil A. and Hussien R. (2015). Vibration analysis of angle-ply laminates composite plate under thermo-mechanical effect. *Journal of Engineering*, vol. 21, no.11, 1-23.
- [3] Sadiq I. and Majeed W. (2018). Thermal buckling of angle-ply laminated plates using new displacement function. *Journal of Engineering*, vol. 25, no. 12, 96-113. <https://doi.org/10.31026/j.eng.2019.12.08>.
- [4] Chen Q., Fei Q., Devriendt H., Wu S., Pluymers B. and Desmet W. (2020). The dynamic bending analysis of plates under thermal load using an efficient wave-based method. *Thin-Walled Structures*, vol. 149, <https://doi.org/10.1016/j.tws.2019.106421>.
- [5] Sator L., Sladek V. and Sladek J. (2019). Coupling effects in transient analysis of FGM plates bending in non-classical thermoelasticity. *Composites Part B: Engineering*, vol. 165, 233-246.
- [6] Dang Z. and Mao Z. (2020). Dynamic response analysis of a thin-walled rectangular plate subjected to thermoacoustic loadings. *archives of thermodynamics*, vol. 41, no. 1, 151–174, DOI: 10.24425/ather.2020.132953.
- [7] Zenkour, A. and El-Shahrany, H. (2021). Hygrothermal vibration of adaptive composite magnetostrictive laminates supported by elastic substrate medium. *European Journal. Of Mechanics - A / Solid*, vol. 85, <https://doi.org/10.1016/j.euromechsol.2020.104140>.
- [8] Bidgoli M., Loghman A., Arefi M., (2019). The effect of grading index on two-dimensional stress and strain distribution of FG rotating cylinder resting on a friction bed under thermomechanical loading. *Journal of Stress Analysis*, vol. 3, no. 2, 75-82.
- [9] Madeh A., Majeed W. (2022). Effect of thermal environment on transient response of laminated shallow shell with different boundary conditions. *Journal of Engineering Science and Technology*, vol. 17, no. 5, 3160 – 3173.
- [10] Majeed W. and Sadiq I. (2023), 'Thermal buckling and stability of laminated plates under non uniform temperature distribution', *Steel and Composite Structures*, vol. 47, no. 4, 503-511 <https://doi.org/10.12989/scs.2023.47.4.503>
- [11] Majeed W. and Tayeh F. (2015). Stability and dynamic analysis of laminated composite plates. *Journal of Engineering*, vol. 21, no. 8, 139.

- [12] Duc N., Tuan N. , Tran P. and Quan T. (2017). Nonlinear dynamic response and vibration of imperfect shear deformable functionally graded plates subjected to blast and thermal loads. *Mechanics of Advanced Materials and Structures*, vol. 24, no. 4, 1-43. <https://doi.org/10.1080/15376494.2016.1142024>.
- [13] Xu Z. and Huang Q. (2019). Vibro-acoustic analysis of functionally graded graphene-reinforced nanocomposite laminated plates under thermal-mechanical loads. *Engineering Structures*, vol. 186, 345-355. <https://doi.org/10.1016/j.engstruct.2019.01.137>.
- [14] Akbas, Seref D. (2020). Dynamic responses of laminated beams under a moving load in thermal environment. *Steel and Composite Structures*, vol. 35, no. 6, 729-737. <https://doi.org/10.12989/scs.2020.35.6.729>.
- [15] Kallannavar V., Kumaran B., Kattimani S. (2020). Effect of temperature and moisture on free vibration characteristics of skew laminated hybrid composite and sandwich plates. *Thin-Walled Structures*, vol. 157, 107-113.
- [16] Malekzadeh P. Monajjemzadeh S. (2012). Dynamic response of functionally graded plates in thermal environment under moving load. *Mechanics of advanced materials and structures*, vol.23, no.3, 248-258. <https://doi.org/10.1080/15376494.2014.949930>.
- [17] Panda S. and Katariya P. (2015). Stability and free vibration behavior of laminated composite panels under thermo-mechanical loading. *International Journal of Applied and Computational Mathematics*, vol. 1, 475–490.
- [18] Chandraa S., Sepahvanda K., Matsagarb V. and Marburga S. (2019). Stochastic dynamic analysis of composite plate with random temperature increment. *Composite Structures*, vol. 226, 1-14. <https://doi.org/10.1016/j.compstruct.2019.111159>.
- [19] Pawlus D. and Fantuzzi N. (2021). Temperature effect on stability of clamped–clamped composite annular plate with damages. *Materials*, vol. 14, no. 16, 1-24. <https://doi.org/10.3390/ma14164559>.
- [20] Pham-Tien, D., Pham-Quoc, H., Vu-Khac T. and Nguyen-Van, N. (2017). Transient analysis of laminated composite shells using an edge-based smoothed finite element method. *International Conference on Advances in Computational Mechanics*, Springer, Singapore, 1075-1094.
- [21] Rivera, M., and Reddy, J. (2017). Nonlinear transient and thermal analysis of functionally graded shells using a seven-parameter shell finite element. *Journal of Modeling in Mechanics and Materials*, vol. 1, no. 2. <https://doi.org/10.1515/jmmm-2017-0003>.
- [22] Sun Y. (2021). Buckling and vibration performance of a composite laminated plate with elastic boundaries subjected to local thermal loading. *Hindawi Shock and Vibration*, vol. 2021, 1-9. <https://doi.org/10.1155/2021/5537946>.
- [23] Bidgoli M., Loghman A., Arefi M. and Faegh R. (2023). Transient stress and deformation analysis of a shear deformable FG rotating cylindrical shell made of AL-SiC subjected to thermo-mechanical loading, *Australian Journal of Mechanical Engineering*, vol.21, no.1, 279-294. DOI: 10.1080/14484846.2020.1842296
- [24] Smaisim G., Bidgoli M., Goh K. and Bakhtiari H. (2022). Review of thermoelastic, thermal properties and creep analysis of functionally graded cylindrical shell. *Australian Journal of Mechanical Engineering*. DOI: 10.1080/14484846.2022.2100045.
- [25] Mantari J., Oktem A., Soares C. (2012). A new higher order shear deformation theory for sandwich and composite laminated plates. *Composites Part B: Engineering*, vol.43, no. 3, 1489-1499. <https://doi.org/10.1016/j.compositesb.2011.07.017>.
- [26] Reddy, J. (2003). *Mechanics of laminated composite plates and shells: theory and analysis*. CRC press. Printed in the united states of America.
- [27] Khdeir A. & Reddy J. (1989). Exact solutions for the transient response of symmetric cross-ply Laminates using a higher-order plate theory. *Composites Science and Technology*, vol. 34, no.3, 205-224. [https://doi.org/10.1016/0266-3538\(89\)90029-8](https://doi.org/10.1016/0266-3538(89)90029-8).
- [28] Khdeir A. and Reddy J. (1988). Dynamic response of antisymmetric angle laminated plates subjected to arbitrary loading. *Journal of sound and vibration*, vol. 126, no. 3, 437-445. [https://doi.org/10.1016/0022-460X\(88\)90222-2](https://doi.org/10.1016/0022-460X(88)90222-2).

Paper submitted: 30.03.2023.

Paper accepted: 29.11.2023.

This is an open access article distributed under the CC BY 4.0 terms and conditions